Astrophysical Phenomena Revealed by Space VLBI
H. Hirabayashi, P.G. Edwards and D.W. Murphy (eds.)

The VSOP Survey II: Reduction Methods

G.A. Moellenbrock[1], J. Lovell[2], S. Horiuchi[3], E. Fomalont[4], H. Hirabayashi[5], R. Dodson[6], S. Dougherty[7], P. Edwards[5], S. Frey[8], L. Gurvits[9], M. Lister[10], D. Murphy[10,5], Z. Paragi[8], G. Piner[10], W. Scott[11], Z. Shen[3], S. Tingay[2], Y. Asaki[5], D. Jauncey[2], G. Langston[1], D. Meier[10], D. Moffet[12], Y. Murata[5], R. Preston[10], R. Taylor[11], K. Wajima[5]

[1]*NRAO, Green Bank, WV, USA*
[2]*ATNF, Epping, NSW, Australia*
[3]*NAO, Mitaka, Tokyo, Japan*
[4]*NRAO, Charlottesville, VA, USA*
[5]*ISAS, Sagamihara, Kanagawa, Japan*
[6]*University of Tasmania, Hobart, Tasmania, Australia*
[7]*DRAO, Penticton, BC, Canada*
[8]*FÖMI, Penc, Hungary*
[9]*JIVE, Dwingeloo, The Netherlands*
[10]*JPL, Pasadena, CA, USA*
[11]*University of Calgary, Calgary, AB, Canada*
[12]*Furman University, Greenville, SC, USA*

Abstract

This second paper on the VSOP Continuum Survey describes the data reduction procedures and gives a sampling of Survey results for individual sources.

1 Data Reduction Procedures

The reduction of VSOP Survey observations is being undertaken by a group of analysts located world-wide. This group has met at ISAS on three occasions and meets regularly via telephone to discuss and formulate procedures for VSOP Survey data reduction and analysis. This section summarizes the data reduction scheme devised for the Survey in these meetings.

1.1 Preliminaries and *a Priori* calibrations.

The Survey observations are undertaken in the standard VSOP observing mode (two 16 MHz two-bit sampled IFs) at sky frequencies in the range 4800–5000 MHz. For initial calibrations and detection of fringes, the correlator distribution data for each experiment is imported into NRAO-AIPS using the task FITLD. The datasets are large: typically 128 frequency channels in each IF, with temporal averaging to 0.5 seconds and 2.0 seconds for space- and ground-baselines, respectively. The datasets are sorted, indexed, and documented using standard AIPS tasks (MSORT, INDXR, LISTR, PRTAN, DTSUM). Except for datasets correlated in Penticton, it is necessary to run ACCOR to remove fringe normalization errors. The *a priori* amplitude calibration is applied using ANTAB to load system temperature and gain values into AIPS tables attached to the dataset, and APCAL to form the $\sqrt{SEFD}$ calibration factors required for each antenna.[1] For HALCA, the nominal 5 GHz system temperature is $\sim$ 90 K and stable. The 5 GHz gain is 0.0062 K/Jy and this yields an $SEFD \sim 14,500$ Jy, which is more than an order of magnitude larger than most ground telescopes. The *a priori* amplitude calibration is thought to be uncertain by 10–20%.

1.2 Fringe-Fitting

Fringe-fitting, where the visibilities are detected, is the most important part of the Survey reductions. Unlike ground-only VLBI, fringe detection for HALCA observations is difficult due to the limited sensitivity of the orbiting station, the generally lower expected correlated flux density and the larger uncertainty in the spacecraft's location and clock. This combination of conditions requires weak-signal fringe searches over large ranges of delay and fringe rate, hence the extremely fine time and frequency sampling. The small number of ground telescopes limits the sensitivity of global fringe-fitting, as well. It is highly desirable to limit as much as possible the range of the search in delay and fringe rate in order to keep the fringe searching efficient, and to avoid false detections. For many Survey datasets, high confidence delay and fringe rate solutions are available from baseline-based fringe searches performed at the correlators for data quality analysis. Application of these solutions

[1] The *System Equivalent Flux Density (SEFD)* is the ratio of the system temperature (K) and telescope gain (K/Jy). It concisely describes the sensitivity of a radio telescope and the geometric mean of $SEFD$ for two telescopes provides the proper scaling factor to convert normalized correlation coefficients to janskys.

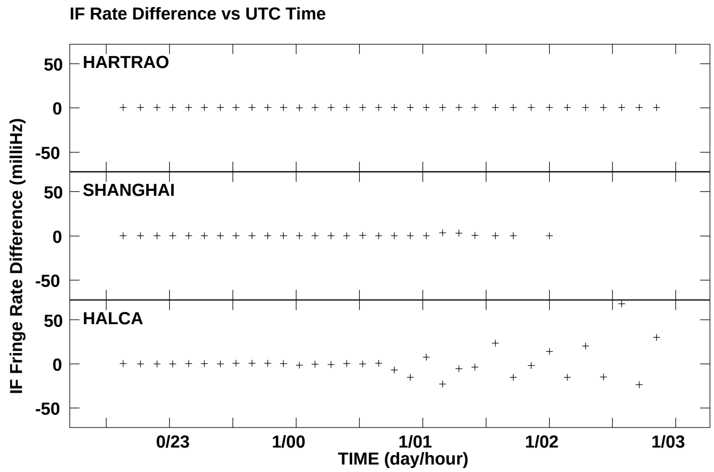

Figure 1: An example of the difference in fringe rate solutions between the two IFs for a typical Survey experiment. Fringes to HALCA are detected until nearly 1/01 at which time the differences become randomly distributed on a scale exceeding the fringe rate resolution (~3 mHz FWHM).

using CLCOR allows significant data averaging and smaller fringe-search windows. For datasets with strong fringes for only a portion of the observation, the resulting narrower search should in principle allow detection of the weaker fringes. In practice, the gains have been modest.

For most observations, the AIPS task FRING is used for fringe-fitting. Solution intervals of at least 10 minutes (approaching the coherence time) are attempted to maximize SNR. Detections are best gauged by consistency in the delay and fringe rate solutions between the two independent IF channels (see Figure 1). For the weakest sources (few or no detections in the correlator's data quality search), the AIPS task KRING may be attempted since it allows larger searches and longer integrations than FRING for the same CPU.

1.3 Imaging and Modelfitting

With limited (u, v)-coverages, the imaging and modelfitting of Survey observations recall the early days of ground-based VLBI imaging. With its simple and efficient implementation, Difmap (Shepherd et al. 1994) has been chosen for post-detection editing, imaging, and modelfitting.

Upon importing the frequency-averaged (each IF) data to Difmap, it is averaged in time to 30-second samples and point-source phase self-calibration solutions are determined on a 10 minute timescale and applied. Manual flags are then applied to obviously discrepant and undetected data, the latter based on lack of continuity in the IF phase solution differences. At this point, the *a priori* amplitude calibration may be checked for consistency using crossing points in the (u, v)-plane (if available) and by comparison with similar baselines from a pre-launch survey (Fomalont et al. 2000). Allowance for source variability is made by assuming the varying part of the source is what dominates the visibilities we measure. The ground array typically observes several calibrator sources (for fringe searching at the correlator), and these provide an amplitude calibration consistency check as well.

Imaging proceeds with incremental and iterative CLEAN deconvolution and phase-only self-calibration. So that the full resolution of the space-VLBI dataset is realized, the HALCA data must be up-weighted by a factor ~20–100 to compensate for their lower sensitivity. The timescale for the self-calibration solutions is limited to the minimum required to maintain clear continuity in the difference of the IF phase solutions. When satisfied with convergence, and if at least four stations are available, constant amplitude self-calibration factors are determined. If the station-based amplitude corrections are less than 10%, the phase-self-calibration imaging is repeated with the new amplitudes and a final image obtained; if not, and if such large discrepancies cannot be accounted for by obvious (if subtle) problems in the *a priori* amplitude calibration, then the phase-only self-calibrated dataset is accepted as the final result. The final calibrated dataset is then modelled with a small number of point and/or Gaussian components. As in the imaging, the HALCA baselines must be up-weighted so that they have a significant influence on the modelfitting solutions.

2 Sample Results

Figure 2 shows the (u, v)-coverages, visibility functions, and images for two typical Survey observations: a northern source (0745+241) observed with the ground telescopes at Mopra, Kashima, and Shanghai and correlated at Mitaka, and a southern source (J0106−4034) observed with Hartebeesthoek and Mopra and correlated at Penticton. The compact component in 0745+241 has a brightness temperature in excess of 0.8×10^{12} K. J0106−4034 is resolved with a peak brightness temperature of $\sim 2.8 \times 10^{12}$ K.

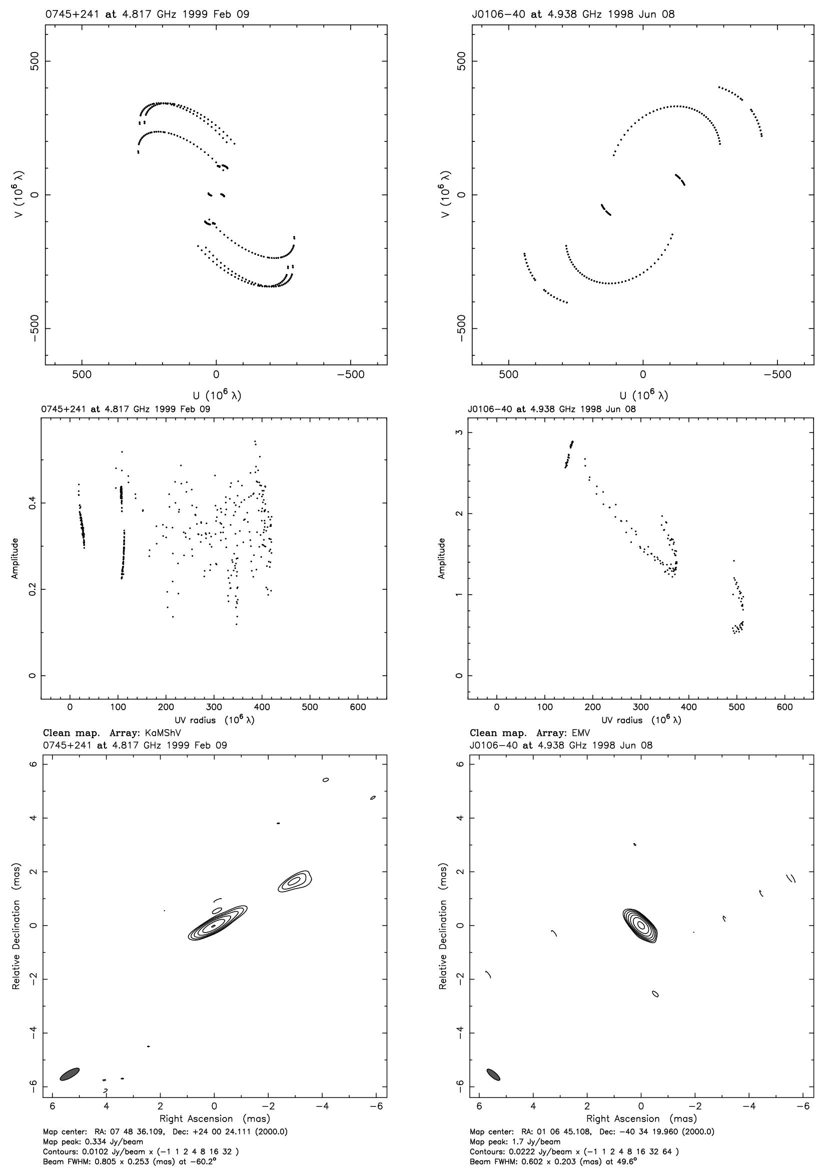

Figure 2: (u, v)-coverages (top), visibility plots (middle) and images for two typical Survey observations: 0745+241 at epoch 1999.11 (left) and and J0106−4034 at epoch 1998.43 (right). For the images, the contour intervals are factors of 2, beginning at ~ 3 times the off-source rms noise (typically 5 mJy/beam) and the full-resolution restoring beam is at the bottom left.

In general, the quality of imaging results rarely approach that which is possible with a full GOT dataset, especially for complex sources; see Lister et al. (these proceedings) for a detailed analysis of the difference between Survey and full GOT datasets. While the Difmap imaging/modelfitting results generally represent the qualitative structure acceptably (familiar sources look familiar), detailed interpretation remains limited. In general, the flux densities and positions of image features below $\sim$15% of the peak carry considerable uncertainty due to the limited (u, v)-coverage. Also, most central modelfitting components are consistent with zero size in at least one dimension, and so a more careful analysis is required to derive robust brightness temperature limits. This issue is discussed in greater detail in Lovell et al. (these proceedings).

Acknowledgements. We gratefully acknowledge the VSOP Project, which is led by the Japanese Institute of Space and Astronautical Science in cooperation with many organizations and radio telescopes around the world. The Australia Telescope National Facility (ATNF) is funded by the Commonwealth of Australia for operation as a National Facility managed by CSIRO. The National Radio Astronomy Observatory is a facility of the U.S. National Science Foundation operated under cooperative agreement by Associated Universities, Inc.

References

Fomalont, E.B. et al., 2000, to be submitted to *AJ*

Shepherd, M.C., Pearson, T.J., & Taylor, G.B. 1994, *BAAS*, **26**, 987